Stable transmission of solitons in the region of normal dispersion

Nikos Efremidis and Kyriakos Hizanidis

Department of Electrical and Computer Engineering, National Technical University of Athens, 9 Iroon Polytexniou, 157 73 Athens, Greece

Boris A. Malomed

Department of Interdisciplinary Studies, Faculty of Engineering, Tel Aviv University, Tel Aviv 69978, Israel

Hector E. Nistazakis and Dimitri J. Frantzeskakis

Department of Physics, University of Athens, Panepistemiopolis, 157 84 Athens, Greece

Received August 9, 1999; revised manuscript received December 16, 1999

We study in detail stability of exact chirped solitary-pulse solutions in a model in which stabilization of the pulses is achieved by means of short segments of an extra lossy core, which is parallel coupled to the main one. We demonstrate that, in the model's three-dimensional parameter space, there is a vast region in which the pulses are fully stable, for both signs of the group-velocity dispersion. These results open the way to a stable transmission of solitary optical pulses in the normal-dispersion region and thus to an essential expansion of the bandwidth offered by the nonlinear optical fibers for telecommunications in the return-to-zero regime. In the cases in which the pulses are unstable, we study the development of the instability, which may end by either blowing up or decaying to zero. In the case when the pulses are stable, we also simulate interactions between them, concluding that they always eventually merge into one pulse. © 2000 Optical Society of America [S0740-3224(00)01606-4]

OCIS code: 060.5530.

1. INTRODUCTION

It is commonly known that solitons may exist in optical fibers in the region of anomalous dispersion.[1] The losses, which are inevitably present in the fibers, can be compensated by the all-optical Er-doped amplifiers.[2] However, the amplifiers also give rise to various instabilities and related detrimental effects, the most dangerous one being a random jitter of the solitons that is induced by their interaction with an optical noise generated by the amplifiers.[3] Schemes providing for stabilization of the transmission of periodically amplified solitons have been successfully developed on the basis of techniques such as guiding (fixed- or sliding-frequency) filters,[4] dispersion management,[5] or a combination of both (see, e.g., Ref. 6).

A basic model that takes into regard the group-velocity dispersion, Kerr's nonlinearity, amplification, and fixed-frequency guiding filters is a perturbed nonlinear Schrödinger (NLS) equation,[3]

$$iu_z + (1/2)Du_{tt} + |u|^2u = iu + iu_{tt}, \qquad (1)$$

where z and t are, as usual, the propagation distance and reduced time and D is the dispersion coefficient (here we do not consider dispersion-management schemes, hence D = const; note that D is defined with a sign opposite that of the frequently used coefficient $\beta^{(1)}$). The nonlinearity coefficient, excess gain, and an effective filtering strength are all normalized to be $\equiv 1$. The gain and filtering terms in Eq. (1) are assumed to be uniformly distributed along the long fiber link. This approximation, which disregards the discrete character of the amplification and filtering, is well justified for the propagation of sufficiently broad solitons (with the temporal width $\tau \gtrsim 10$ ps), whose soliton period z_0 is essentially larger than the amplification spacing z_a (Ref. 3).

Until the change of the notation, Eq. (1) is simultaneously a particular case of the complex cubic Ginzburg–Landau (GL) equation, which is a well-known paradigm model in the nonlinear pattern-formation theory.[7] It is well known that the GL equation (1) has an exact pulse solution,[8] which describes a stationary solitary pulse with an internal chirp. It is necessary to stress that, while the unperturbed NLS equation, i.e., Eq. (1) without the right-hand side, has (bright) soliton solutions only in the case of anomalous dispersion, $D > 0$, the full GL equation (1) has the exact solitary-pulse solution in all the cases (also when the coefficient in front of the cubic term is complex, taking into regard two-photon absorption, although in the present paper the latter coefficient is assumed to be real). An explanation for this property is that, whereas in the case of the unperturbed NLS equation the compensation between nonlinearity and dispersion is possible only when the dispersion is anomalous, in the case of the GL equation the nonlinearity, dispersion, and filtering may all be in balance through the internal chirp of the stationary soliton.

A fundamental drawback of the exact pulse solution to Eq. (1) is that it is unstable, as the zero solution is unstable against perturbations of the form $u \sim \exp(-i\omega t)$

with $\omega^2 < 1$. This instability reflects a fundamental problem that exists in systems in which the transmission of solitons is supported by means of a distributed linear gain. However, the rate at which the instability grows and eventually destroys the pulse strongly depends (for a fixed level of initial small perturbations that are amplified by the instability) on the relation between dispersion and filtering, i.e., on the value (and sign) of the coefficient D in Eq. (1). Recently, this issue was investigated by means of direct numerical simulations in Ref. 9. It was demonstrated that, in the case of the normal dispersion, $D < 0$, the distance $z_{\rm stab}$ of the stable propagation (followed by an instability-induced blowup) is much larger (by a factor of as great as ~100) than in the anomalous-dispersion case. The distance $z_{\rm stab}$ reaches a maximum at D close to an optimum value, $D_{\rm opt} \approx -18$, and then gradually decreases with the further increase of $|D|$ inside the normal-dispersion region.

Thus quasi-stable transmission of pulses in the normal-dispersion range of the carrier wavelengths is possible and may actually be more stable than in the anomalous-dispersion range. Besides better stability, employing the normal-dispersion range has another obvious advantage, the ability to use a broader wavelength band in the return-to-zero (i.e., solitary-pulse-based) communication mode.

Nevertheless, full stability of the pulses cannot be achieved within the framework of the model [Eq. (1)]. An approach allowing one to suppress the instability of the zero state and thus open the way to the generation of completely stable solitary pulses was proposed in Ref. 10 and then checked by means of direct simulations in Ref. 11: One should linearly couple the fiber to an additional parallel lossy core (for the first time, a similar idea was proposed in Ref. 12 as a filter improving the operation of a fiber-loop laser). It should be stressed that there is no need to actually replace the usual single-core telecommunication fibers by the dual-core ones. In reality, one can add short segments of the parallel lossy core, integrating them with the amplifiers and filters periodically installed into the fiber link. The simplest possibility is to use dual-core Er-doped optical amplifiers, with both cores doped and only one core that is pumped by an external source of light. The unpumped dopants in the second core will give rise to strong resonant losses instead of a gain. Then, in the above-mentioned usual case, $z_0 \gg z_a$, the application of the well-known guiding-center approximation[3] allows one to treat the extra core in the uniformly distributed approximation, as is usually done with the gain and filtering.

To estimate the actual length l of the short segments of the parallel core, we note that, upon the averaging along the fiber link, an effective coupling coefficient K between the core is $(l/z_a)K_0$, where K_0 is its actual local value (recall we assume that the additional segments are inserted with the spacing z_a between them). Consequently, an effective coupling length Λ (Ref. 13) between the two cores in the uniformly distributed approximation is $\Lambda \sim 1/K \sim (z_a/l)\Lambda_0$, where $\Lambda_0 \sim 1/K_0$ is the actual coupling length in the dual-core fiber (usually, $\Lambda_0 \sim 10$ cm).[13] On the other hand, the extra core plays a nontrivial role if the effective coupling length is of the same order of amplitude as the soliton period.[10,11] Thus we arrive at a condition $(z_a/l)\Lambda_0 \sim z_0$, which finally predicts the necessary length of the dual-core fiber segments, $l \sim (z_a/z_0)\Lambda_0$, which implies the length of a few centimeters. Note that the additional core may actually be essentially longer, so that only its very short segment of the length l is coupled to the main core, while the rest is a loose piece of the fiber that provides for the dissipation of the light coupled into the lossy core.[12]

The system with the extra lossy core is bistable: It has two stable states (attractors) in the form of the zero solution and a nontrivial solitary pulse with uniquely determined parameters, which are separated by an unstable pulse solution with a smaller amplitude and larger width. Later, it was demonstrated[14] that the stable pulse in this dual-core model can be found in an exact form. However, the numerical stability analysis of the pulses performed in Ref. 14 was rather sketchy and comprised limited parametric regions. In this paper our aim is to develop a systematic analysis of the pulse transmission in the model stabilized by means of the parallel lossy core. We will demonstrate that absolutely stable pulses can propagate at both normal and anomalous values of the dispersion, which opens the way for a more efficient use of the fiber's bandwidth in the wavelength division multiplexing mode.[15]

The rest of the paper is organized as follows. In Section 2 we formulate the model and describe its exact solitary-pulse solution. In Section 3 we perform a systematic analysis of the stability of the zero solution in the model, which provides for a necessary basis for the direct numerical analysis of the soliton's stability in Section 4. The main result of Section 4 is a three-dimensional picture that shows a full stability region in the model's parameter's space. In Section 5 we study interactions between two stable pulses separated by some distance (actually, by a temporal delay). The result is that, irrespective of the initial phase difference between the pulses, they eventually merge into a single one. Section 6 concludes the paper.

2. MODEL

Two parallel-coupled cores are described in the uniformly distributed approximation (see above) by a system of normalized equations of the following form[14] [cf. Eq. (1)]:

$$iu_z + (\tfrac{1}{2}D - i)u_{tt} + |u|^2u - iu = Kv, \tag{2}$$

$$iv_z + i\Gamma v + k_0 v = Ku. \tag{3}$$

Here u and v are the field amplitudes in the main core and in the extra one, with a loss constant Γ in it; K is a coupling constant; and k_0 is a phase-velocity mismatch between the two cores. As it is demonstrated in Refs. 11 and 14, the nonlinearity and dispersion in the additional core may be neglected, and the filtering inside it, as well a possible group-velocity mismatch between the cores, also produces inconsiderable effects that are neglected in Eq. (3). In Eq. (2) the filtering coefficient and the excess gain, which is necessary to compensate the losses induced by the filtering and the lossy core, are normalized to be 1 [it is assumed, as usual, that the basic frequency-

independent losses in the fiber are compensated by the main part of the gain, both terms not appearing in Eq. (2) explicitly].

To estimate relevant values of the renormalized parameters in the model, we recall that the gain bandwidth of the Er-doped optical amplifier, which produces the gain, is $\Delta\omega \sim 1$ THz (Ref. 2) and a typical value of the fiber losses is $|\gamma| \approx 0.05\,\mathrm{km}^{-1}$, so that a minimum value of the physical filtering coefficient (which corresponds to the finite gain bandwidth, without the filters proper) can be estimated as $\gamma_2 = \gamma/(\Delta\omega)^2 \sim 0.05\,\mathrm{ps}^2/\mathrm{km}$. A typical value of the physical dispersion coefficient in the telecommunication fibers is $|\beta_2| = 20\,\mathrm{ps}^2/\mathrm{km}$ (Ref. 1); hence the relative dispersion coefficient in Eq. (2), $D \equiv \beta_2/\gamma_2$, takes values within a broad interval $|D| \leqslant 400$.

The system of Eqs. (2) and (3) possesses an exact analytical solution[14] that follows the pattern of the original solitary-wave solution to Eq. (1),[8]

$$u = u_0 \exp(ikz)[\mathrm{sech}(\eta t)]^{(1+i\mu)}, \tag{4}$$

$$v = v_0 \exp(ikz)[\mathrm{sech}(\eta t)]^{(1+i\mu)}, \tag{5}$$

where the chirp parameter μ is

$$\mu = -(3/4)D + (1/4)\sqrt{32 + 9D^2} \tag{6}$$

and the amplitudes u_0 and v_0 in the gain- and loss-cores are linearly related,

$$v_0 = (k_0 - k + i\Gamma)^{-1} K u_0, \tag{7}$$

while the remaining parameters u_0, η, and k are determined as follows. First, the relative phase-velocity mismatch $\delta = k_0 - k$ must be found from a cubic equation:

$$-(\mu D - 2)\delta^3 + [(1-\mu^2)D + 4\mu + k_0(\mu D - 2)]\delta^2 + (\mu D - 2)(K^2 - \Gamma^2)\delta + [(1-\mu^2)D + 4\mu] \times \Gamma(\Gamma - K^2) + (\mu D - 2)k_0\Gamma^2 = 0. \tag{8}$$

Second, the soliton's inverse width η is given by

$$\eta^2 = \frac{\delta(1-\Gamma) + k_0\Gamma}{\delta(2 - D\mu) + \Gamma[D(1-\mu^2) + 4\mu]}, \tag{9}$$

and, finally, the amplitude u_0^2 is determined by the expression

$$u_0{}^2 = (3/4)\mu(4 + D^2)\eta^2. \tag{10}$$

Physical solutions to the cubic equation (8) are those that yield $\eta^2 > 0$.

Thus an exact analytical solution in the form of a chirped solitary pulse is available in the present model. However, we will see in the following sections that the stability analysis for this solution is a fairly complicated problem, which can be solved only numerically.

3. STABILITY OF THE ZERO SOLUTION

Proceeding to the stability analysis, we first notice that the solitary pulse [Eqs. (4) and (5)] cannot be stable unless its background (i.e., the zero solution, $u = 0$, $v = 0$) is stable. Recall that it is exactly the instability of the zero solution that renders unstable all solitary-pulse solutions to the GL equation (1).

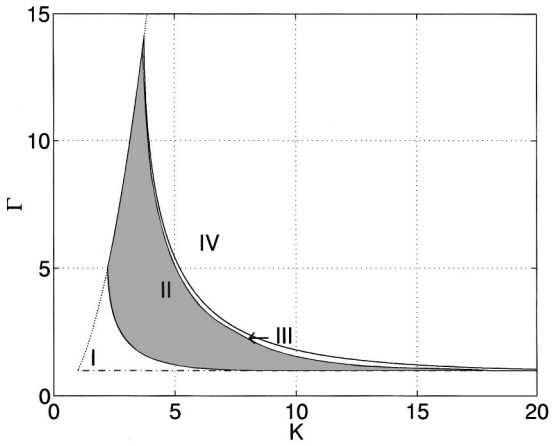

Fig. 1. Regions of the stability of the zero solution and regions of the existence and stability of the exact solitary-wave solution in the (Γ, K) parameter plane in the dual-core model. Region I: The zero solution is unstable. Region II: The solitary-wave solution is stable. Region III: The zero solution is stable, while the solitary-wave solution is not, showing a decay into zero. Region IV: The solitary-wave solution does not exist. Note that, outside region I, which is bounded by the curves $\Gamma = K^2$ (dotted curve) and $\Gamma = 1$ (dotted–dashed curve), the zero solution is unstable [see relation (13)].

To investigate the stability of the zero solution, we linearize Eqs. (2) and (3), substituting into them infinitesimal perturbations

$$u = u_1 \exp[i(kz - \omega t)], \qquad v = v_1 \exp[i(kz - \omega t)], \tag{11}$$

where k and ω are the (complex) wave number and (real) frequency of the perturbations, respectively. Then the stability region in the plane of the model's parameters (Γ, K) is determined by the condition $\mathrm{Im}\,k \geqslant 0$, which, after some algebra, leads to the inequality

$$K^2 \geqslant \Gamma(1 - \omega^2)\left[1 + \frac{(2k_0 + D\omega^2)^2}{4(\Gamma - 1 + \omega^2)^2}\right]. \tag{12}$$

Evidently, this inequality always holds at $\omega^2 \geqslant 1$. Therefore we need to consider relation (12) only for $\omega^2 < 1$. Additionally, it is readily seen that the condition $\Gamma > 1$ must hold for the right-hand side of relation (12) to remain finite at these values of ω. In the case $\omega^2 < 1$, relation (12) can be strongly simplified in some special cases, e.g., when $k_0 = D = 0$, or $\Gamma \gg 1$, or $k_0 = \omega = 0$, reducing to

$$1 < \Gamma < K^2. \tag{13}$$

This is a known condition[10,11,14] that defines an area in the (K, Γ) plane, limited by two curves shown in Fig. 1, $\Gamma = K^2$ and $\Gamma = 1$, where the trivial solution is stable in the above-mentioned special cases.

In what follows below, we will chiefly concentrate on the most straightforward case $k_0 = 0$ (which corresponds, in particular, to the above-mentioned configuration when the two cores are identical, the asymmetry between them being created by the fact that only in one core is the resonant dopant pumped by an external source of light), although changes brought about by $k_0 \neq 0$ will also be considered.

Setting $k_0 = 0$, we will fix D, aiming to analyze the stability condition (12) in the (Γ, K) plane. As for the choice

of the value of D, it was mentioned above[9] that, in the case of the single GL equation (1), the propagation distance z_{stab} before the onset of the soliton's instability took its maximum value around $D = -18$; hence it seems natural to dwell first on this value.

On investigating the condition (12) numerically, we have found, varying the arbitrary real frequency ω, that there exists a hyperbolalike curve, which further reduces the stability region of the zero solution defined by relation (13) (namely, the corner region I is excluded), as is shown in Fig. 1. It is noted that, for large values of Γ, this numerically found curve coincides with the one for which $\Gamma = K^2$, whereas for large values of K, it asymptotically approaches the straight line $\Gamma = 1$; see Fig. 1.

4. STABILITY OF THE SOLITARY PULSES

Proceeding from the stability conditions for the zero solutions to the full stability analysis for the solitary-pulse solutions given by Eqs. (4) and (5), one should first isolate a region in the (Γ, K) plane where these solutions actually exist. The existence condition may be readily found upon utilizing Eq. (8), which may have one or three real solutions for k that determine the soliton's inverse width η [see Eq. (9)]. The condition $\eta^2 > 0$ selects physical solutions of the cubic equation (8). Following this method, we have numerically found that there is an additional hyperbolalike curve (a border between regions III and IV in Fig. 1) in the (Γ, K) plane, below which the existence of at least one real positive value of η^2 is guaranteed. Beyond this curve, there exists a region IV, where the solutions given by Eqs. (4) and (5) cease to exist.

Thus we have found a finite, boomerang-shaped region in the (Γ, K) plane (regions II and III, Fig. 1), where the two conditions, viz., the stability of the zero solution and the existence of the exact solitary-wave one, are satisfied. However, direct numerical simulations of the solitary pulse's evolution demonstrate that it is really stable only in the shaded portion (region II), in the currently considered case $D = -18$ (and $k_0 = 0$). In contrast, in the slim region III the solitary solutions are unstable. Inside region II, the pulse is found to be completely stable over indefinitely long propagation distances. In Fig. 2 we display a typical example of a robust pulse found for $K = 5$ and $\Gamma = 4$ (this point is located approximately in the center of the stability region in Fig. 1).

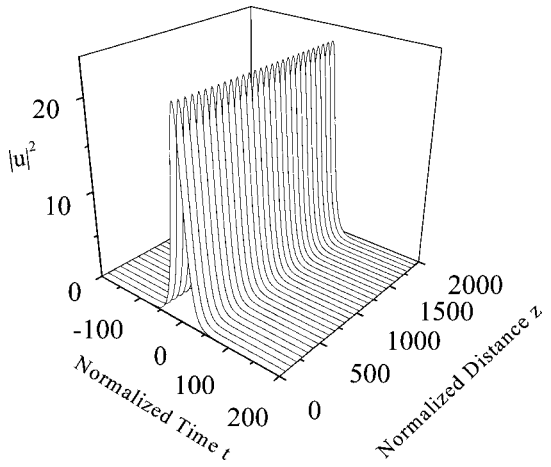

Fig. 2. Evolution of a stable pulse in the case $D = -18$, $k_0 = 0$, and $(K, \Gamma) = (5,4)$, corresponding to region II in Fig. 1.

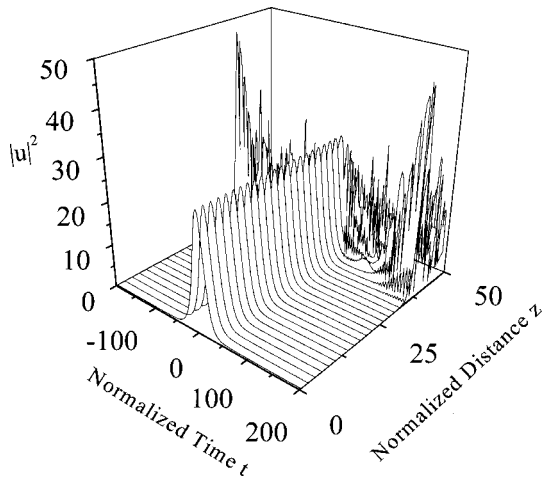

Fig. 3. Evolution of an unstable pulse in the case $D = -18$, $k_0 = 0$, and $(K, \Gamma) = (1.5, 1.5)$, corresponding to region I in Fig. 1. In this case, an initially laminar propagation of the pulse ends with a blowup.

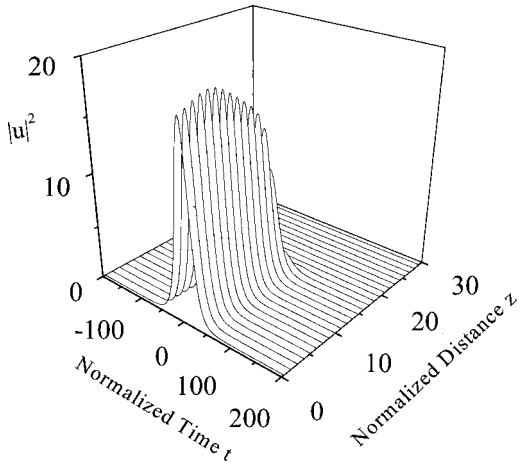

Fig. 4. Evolution of an unstable pulse in the case $D = -18$, $k_0 = 0$, and $(K, \Gamma) = (6.2, 3.6)$, corresponding to region III in Fig. 1. In this case, the initially laminar propagation of the pulse ends with a decay into zero.

Inside region I, as we have seen, the zero solution is unstable. As is illustrated by Fig. 3 for $K = 1.5$ and $\Gamma = 1.5$, in this case the "laminar" evolution of the pulse is eventually followed by a blowup. Comparison with the results of Ref. 9 demonstrates that the propagation distance z_{stab} before the onset of the blowup in the present dual-core model is approximately an order of magnitude larger than in the single-core one at the same values of the common parameters of the two models.[9] The further one moves away from region II (deeper into region I), the wider the range of frequencies that generate the instability becomes, resulting in a decrease of the quasi-stable propagation distance.

Inside region III, the pulse decays to zero. In Fig. 4 we display a typical example of such a case for $K = 6.2$ and $\Gamma = 3.6$: The pulse propagates initially with small

changes in its shape, but then it rapidly decays to nothing, in compliance with the fact that the zero solution is stable in this region.

Figure 5 summarizes the stability of the solitary-wave solutions, along with the stability of the zero background, as one varies the coupling parameter K at fixed values of the other parameters, namely, $\Gamma = 3$, $D = -18$, and $k_0 = 0$. In this figure the peak powers ${u_0}^2 \equiv |u(t=0)|^2$ of the solutions are plotted versus K. The thin dashed curve corresponds to a root of the cubic equation (8) that gives $|u_0|^2 < 0$; this solution is thus theoretical. However, there are two other roots of the cubic equation leading to positive $|u_0|^2$, which correspond to solutions that are either stable (the solid curve) or unstable (the heavy dashed curve).

Coming back to the four regions distinguished in Fig. 1, we conclude that, inside region I, both the zero and the solitary-wave solutions are unstable. Then as K is increased, we cross into region II, where there exist both stable and unstable solitary-wave solutions, the zero solution being stable. In this region the stable soliton, along with the stable zero background, acts as an attractor for the unstable solitary-wave solution: Simulations demonstrate that there is a subregion II(a) (shown in Fig. 5) in which the unstable pulse evolves into the stable trivial solution, while in another subregion II(b) (shown in Fig. 5), it evolves into the stable pulse. Lastly, in region III, both solitary-wave solutions are unstable and collapse into the zero solution. Note that the upward and downward arrows in Fig. 5 indicate the direction of the attraction.

So far, we analyzed the stability of the solitary wave for the fixed values $D = -18$ and $k_0 = 0$. To investigate the change of the stability region with varying D and k_0, we may evaluate numerically the area of the stability region for the solitary pulse on the (K, Γ) plane, upon determining the boundary curves separating regions I, II and III, IV. The results are shown in Fig. 6, where the stability region's area is plotted versus D for $k_0 = -1, 0, 0.5, 1$. As can be seen, in the case $k_0 = 0$ the stability area is an even, parabolalike function of D that increases with $|D|$.

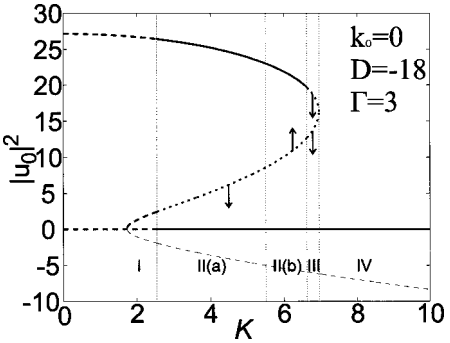

Fig. 5. Peak power of the solitary-wave solution versus the coupling parameter K for $\Gamma = 3$, $D = -18$, and $k_0 = 0$. The thin dashed curve corresponds to an unphysical solitary-wave solution [the root of the cubic equation (8) gives $|u_0|^2 < 0$ in this case]. The heavy solid and dashed curves correspond to physically existing stable and unstable solutions (including both the solitary-pulse and the zero solutions), respectively. The upward and downward arrows indicate the direction of a transition from the unstable solution to a stable one.

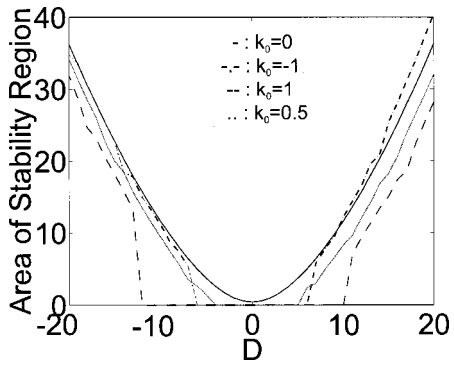

Fig. 6. Area of the stability region of the solitary-wave solution [in the plane (K, Γ)] versus D for $k_0 = -1,0,0.5,1$.

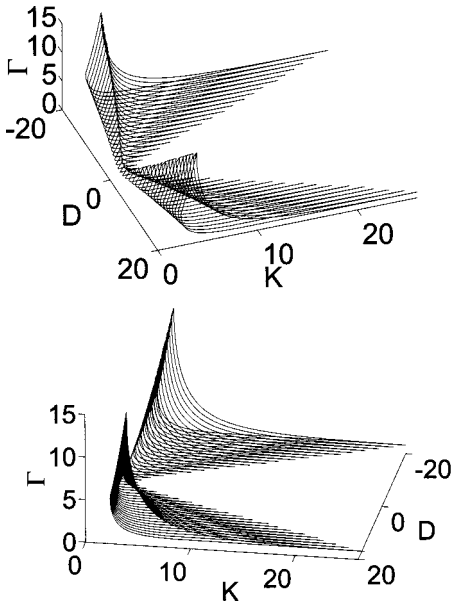

Fig. 7. Stability region of the exact solitary-pulse solutions of the dual-core model in the three-dimensional parameter space (K, D, Γ). The stability region is bounded by the surface shown from two different directions.

As we increase k_0 to positive values ($k_0 = 0.5$ or 1), the stability area monotonically decreases, creating an interval around $D = 0$ where all the solutions are unstable. On the other hand, if we decrease k_0 to negative values, the stability area does not decrease monotonically. In particular, for $k_0 = -1$, it is observed that, for $D \gtrsim 10$, the stability area is increased, while for negative values $D \lesssim -7$, it almost coincides with that corresponding to $k_0 = 0$.

Coming back to the most essential case $k_0 = 0$, we can collect all the data concerning the stability of the exact solitary-pulse solutions in the form of a three-dimensional picture displayed in Fig. 7. This figure shows the stability region in the parameter space (K, D, Γ) from two different directions in this space. This result, showing fairly large stability regions at positive and negative D (i.e., anomalous and normal group-velocity dispersion in the main core) is the main result of this work.

To conclude this section, it is relevant to stress that we analyzed only the stability of the exact pulse solution. It is not ruled out that the same model may have other

pulse solutions that are not given by exact analytical expressions. Consideration of this issue is, however, beyond the scope of the present work.

5. INTERACTION BETWEEN THE STABLE PULSES

When stable solitary pulses are found, it is natural to study their interactions. We do this by simulating configurations defined by the following initial condition for Eqs. (2) and (3):

$$u = u_0 \operatorname{sech}\left[\eta\left(t - \frac{\tau}{2}\right)\right]^{1+i\mu} + u_0 \operatorname{sech}\left[\eta\left(t + \frac{\tau}{2}\right)\right]^{1+i\mu} \exp(i\phi), \tag{14}$$

$$v = v_0 \operatorname{sech}\left[\eta\left(t - \frac{\tau}{2}\right)\right]^{1+i\mu} + v_0 \operatorname{sech}\left[\eta\left(t + \frac{\tau}{2}\right)\right]^{1+i\mu} \exp(i\phi). \tag{15}$$

Equations (14) and (15) represent two pulses in each core, with a temporal separation τ and phase difference ϕ between them. The pulses evolve without tangible changes in their shape and separation, before their collision almost instantly takes place. Apparently, the collision is a result of attraction between the pulses. As is seen in a typical example displayed in Fig. 8, the interaction results in a merger of the two initial pulses into a single one, which finally relaxes into a stationary pulse, virtually coinciding with the exact solution given by Eqs. (4) and (5). In this example we have $K = 5$ and $\Gamma = 4$, while the initial pulse separation and phase difference are $\eta\tau = 8$ and $\phi = 0$. As one can see in Fig. 8, the interaction of the pulses' tails in the region between them generates local peaks and dips (due to the presence of the chirp in each pulse) that tend to increase along with the propagation distance. Actually, the interaction does not seem to change the initial shapes of the pulses significantly up to the point $z = 490$, at which the two pulses begin to really interact and quickly merge into one stable pulse at $z = 520$.

The aforementioned normalized values have a direct practical application to optical transmission systems. Typically, the amplifier span and the amplifier length have the values $z_a = 40\,\mathrm{km}$ and $L_a = 100\,\mathrm{m}$, respectively, while the fiber loss is $\gamma = 0.2\,\mathrm{dB/km}$ $(0.05\,\mathrm{km}^{-1})$ and the amplifier gain is $g = 0.08\,\mathrm{dB/m}$ $(20\,\mathrm{km}^{-1})$. Thus, taking into account that the propagation distance z is normalized to $L = z_a/L_a g$, we conclude that a unit of the normalized z corresponds to 20 km. This means that the collision distance of the two solitary pulses shown in Fig. 8 is ≈10,000 km (which implies that the collisions and the merger of the two pulses into one are not critically dangerous: The collision distance may exceed the actual transmission distance). In addition, assuming that the filtering coefficient γ_2 has a typical value -0.05 $\mathrm{ps}^2/\mathrm{km}$ and taking into account that the time t is normalized to $T = (\gamma_2 z_a/gL_a)^{1/2}$, we conclude that a normalized unit of t corresponds to 1 ps. This implies that the full width at half-maximum (FWHM) of the solitary pulses displayed in Fig. 8 is ≈25 ps, while the temporal separation between them is $\tau \simeq 130\,\mathrm{ps}$. Finally, it should be mentioned that the dispersion coefficient $\beta_2(\equiv D\gamma_2)$ corresponding to $D = -18$ is found to be 0.9 $\mathrm{ps}^2/\mathrm{km}$, which means that the carrier wavelength is close to the zero-dispersion point of the dispersion-shifted fiber.

As the initial separation $\eta\tau$ is increased, the collision distance (i.e., the distance after which the attraction becomes tangible) is found to grow exponentially, as is shown in Fig. 9. The initial phase difference ϕ does not significantly affect the interaction, the collision distance only slightly varying with ϕ; see Fig. 9. Moreover, even in the case $\phi = \pi$, when the usual NLS solitons are known to repel each other,[1] the chirped stable pulses existing in the present model again merge into a new single one; see Fig. 10.

The interaction between the pulses leading into their merger causes, of course, a very detrimental effect for the information transmission, but, using the data presented in Fig. 9, one can easily select parameters of the communication system operating in the return-to-zero regime so that the collision distance will be much larger than the

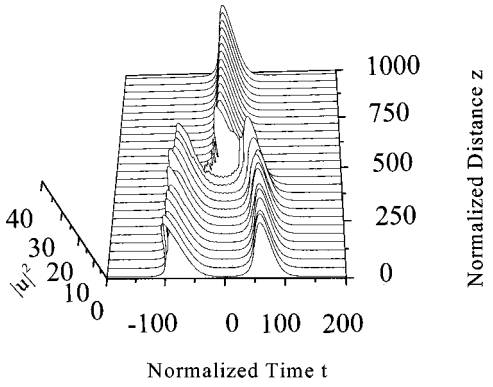

Fig. 8. Interaction of two solitons at $K = 5$ and $\Gamma = 4$. The initial normalized pulse separation and phase difference are $\eta\tau = 8$ and $\phi = 0$, respectively.

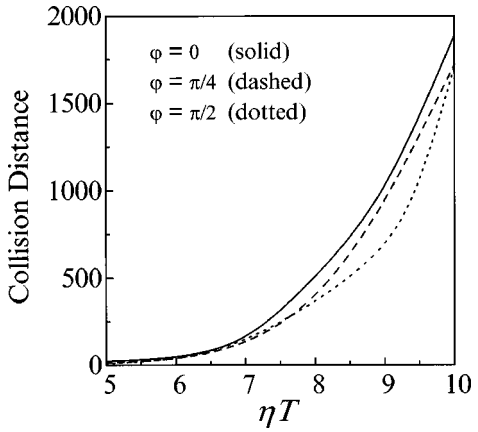

Fig. 9. Collision distance as a function of the normalized initial pulse separation $\eta\tau$, for several values of the initial phase difference: $\phi = 0, \pi/4, \pi/2$.

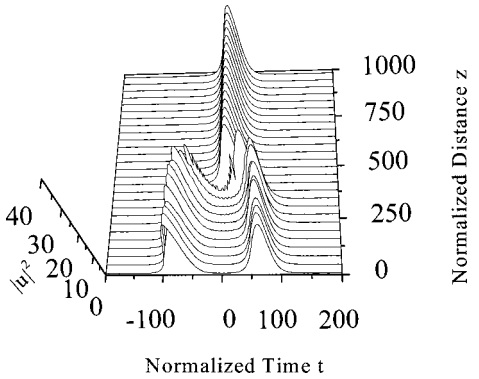

Fig. 10. Merger of two chirped solitons into one in the case when the initial pulse and phase separations are $\eta\tau = 8$ and $\phi = \pi$.

actual distance of the solitons' propagation; hence the merger will not take place.

6. CONCLUSION

In this paper we have studied in detail stability of exact chirped solitary-pulse solutions in a model in which stabilization of the pulses is achieved by means of short segments of an extra lossy core that is parallel coupled to the main one. We have demonstrated that, in the model's three-dimensional parameter space, there is a vast region where the pulses are fully stable, for both signs of the group-velocity dispersion, normal and anomalous. These results open the way to a stable transmission of optical solitons in the normal-dispersion region and thus to an essential expansion of the bandwidth offered by the nonlinear optical fibers for telecommunications. In the cases in which the pulses are unstable, we have studied in detail the development of the instability, which may end up by either blowing up or decaying into zero.

ACKNOWLEDGMENTS

This paper was supported by the General Secretariat of Research and Technology of the Hellenic Ministry of Development (PENED-95 grants 1242 and 644) and by the Special Research Account of the University of Athens.

REFERENCES

1. G. P. Agrawal, *Nonlinear Fiber Optics* (Academic, San Diego, 1995).
2. E. Desurvire, *Erbium-Doped Fiber Amplifibers* (Wiley, New York, 1994).
3. A. Hasegawa and Y. Kodama, *Solitons in Optical Communications* (Oxford U. Press, Oxford, UK, 1995).
4. A. Mecozzi, J. D. Moores, H. A. Haus, and Y. Lai, "Soliton transmission control," Opt. Lett. **16**, 1841–1843 (1991); Y. Kodama and A. Hasegawa, "Generation of asymptotically stable optical solitons and suppression of the Gordon–Haus effect," Opt. Lett. **17**, 31–33 (1992).
5. A. Hasegawa, Y. Kodama, and A. Maruta, "Recent progress in dispersion-managed soliton transmission technologies," Opt. Fiber Technol. Mater. Devices Syst. **3**, 197–213 (1997).
6. M. Matsumoto, "Theory of stretched-pulse transmission dispersion-managed fibers," Opt. Lett. **22**, 1238–1240 (1997); B. A. Malomed, "Jitter suppression guiding filters in combination with dispersion management," Opt. Lett. **23**, 1250–1252 (1998); A. Berntson and B. A. Malomed, "Dispersion management with filtering," Opt. Lett. **24**, 507–509 (1999).
7. M. C. Cross and P. C. Hohenberg, "Pattern formation outside of equilibrium," Rev. Mod. Phys. **65**, 851–1112 (1993).
8. L. M. Hocking and K. Stewartson, "On the nonlinear response of a marginally unstable plane parallel flow to a two-dimensional disturbance," Proc. R. Soc. London, Ser. A **326**, 289–313 (1972); N. R. Pereira and L. Stenflo, "Nonlinear Schroedinger equation including growth and damping," Phys. Fluids **20**, 1733–1734 (1977).
9. B. A. Malomed, D. J. Frantzeskakis, H. E. Nistazakis, A. Tsigopoulos, and K. Hizanidis, "Dissipative solitons under the action of third-order dispersion," Phys. Rev. E **60**, 3324–3331 (1999).
10. B. A. Malomed and H. G. Winful, "Stable solitons in two-component active systems," Phys. Rev. E **53**, 5365–5368 (1996).
11. J. Atai and B. A. Malomed, "Stability and interactions of solitons in two-component active systems," Phys. Rev. E **54**, 4371–4374 (1996).
12. H. G. Winful and D. T. Walton, "Passive mode locking through nonlinear coupling in a dual-core fiber laser," Opt. Lett. **17**, 1688–1690 (1992); D. T. Walton and H. G. Winful, "Passive mode locking with an active nonlinear directional coupler: positive group-velocity dispersion," Opt. Lett. **18**, 720–722 (1993).
13. A. W. Snyder, D. J. Mitchell, L. Poladian, D. R. Rowland, and Y. Chen, "Physics of nonlinear fiber couplers," J. Opt. Soc. Am. B **8**, 2102–2118 (1991).
14. J. Atai and B. A. Malomed, "Exact stable pulses in asymmetric linearly coupled Ginzburg–Landau equations," Phys. Lett. A **246**, 412–422 (1998).
15. L. F. Mollenauer, S. G. Evangelides, and J. P. Gordon, "Wavelength division multiplexing with solitons in ultra-long distance transmission using lumped amplifiers," J. Lightwave Technol. **9**, 362–367 (1991); P. V. Mamyshev and L. F. Mollenauer, "Wavelength-division-multiplexing channel energy self-equalization in a soliton transmission line by guidings," Opt. Lett. **21**, 1658–1660 (1996).